Supplementary information for:

Collagen-inspired biomimetic peptides as therapeutic agents against methylglyoxal-mediated damage

Sergio D. Garcia Schejtman[1†], Juan D. Figueroa Alegria[1†], Ramis Ileri[1,2†], Micaela Giannetti[1], Jessica Hernandez Juarez[1,2], Bryan Liu[1], Emilio I. Alarcon[1,2,3*], and Erik J. Suuronen[1,2,4*]

[1] Bioengineering and Therapeutic Solutions (BEaTS) Research, Division of Cardiac Surgery, University of Ottawa Heart Institute, 40 Ruskin Street, Ottawa, Ontario, Canada, K1Y 4W7.

[2] Ottawa-Carleton Institute for Biomedical Engineering, University of Ottawa, 800 King Edward Avenue, Ottawa, Ontario, Canada, K1N 6N5.

[3] Department of Biochemistry, Microbiology, and Immunology, University of Ottawa, Ottawa, Ontario, Canada, K1H 8M5.

[4] Department of Cellular and Molecular Medicine, University of Ottawa, Ottawa, Ontario, Canada, K1H 8M5.

[†] These authors contributed equally.

***Corresponding authors**: ealarcon@uottawa.ca & esuuronen@ottawaheart.ca

Index	
	Page S

Supplementary Table 1. Collagen-like peptide (CLP) library. For each peptide code, the table lists the full sequence (N → C), the peptide purity determined by analytical HPLC-DAD-MS, and the ratio of the positive peak intensity to the negative peak intensity (Rpn) calculated from CD spectra.

Code	Sequence	Purity (%)	Rpn ± SD [a]
Pep1	H_2N-GGG**(POG)$_6$**GGG-OH	98	0.057 ± 0.002
Pep2	H_2N-G**R**G**(POG)$_6$**GGG-OH	99	0.052 ± 0.002
Pep3	H_2N-GGG**(POG)$_6$**G**R**G-OH	99	0.085 ± 0.002
Pep4	H_2N- GGG**(POG)$_2$(P**R**G)(POG)$_3$**GGG-OH	98	0.041 ± 0.002
Pep5	H_2N-**RR**G**(POG)$_6$**GGG-OH	99	0.060 ± 0.001
Pep6	H_2N-G**R**G**(POG)$_6$**G**R**G-OH	99	0.071 ± 0.002
Pep7	H_2N-GGG**(POG)$_6$**G**RR**-OH	98	0.056 ± 0.004
Pep8	H_2N-**RRR(POG)$_6$**GGG-OH	98	0.081 ± 0.001
Pep9	H_2N-**RR**G**(POG)$_6$**G**R**G-OH	98	0.051 ± 0.002
Pep10	H_2N-G**R**G**(POG)$_6$**G**RR**-OH	98	0.052 ± 0.003
Pep11	H_2N-GGG**(POG)$_6$RRR**-OH	98	0.064 ± 0.005
AcPep1	**Ac**-GGG**(POG)$_6$**GGG-OH	98	0.060 ± 0.002
AcPep2	**Ac**-G**R**G**(POG)$_6$**GGG-OH	98	0.090 ± 0.003
AcPep3	**Ac**-GGG**(POG)$_6$**G**R**G-OH	98	0.071 ± 0.005
AcPep8	**Ac-RRR(POG)$_6$**GGG-OH	98	0.057 ± 0.001
AcPep11	**Ac**- GGG**(POG)$_6$RRR**-OH	98	0.061 ± 0.001

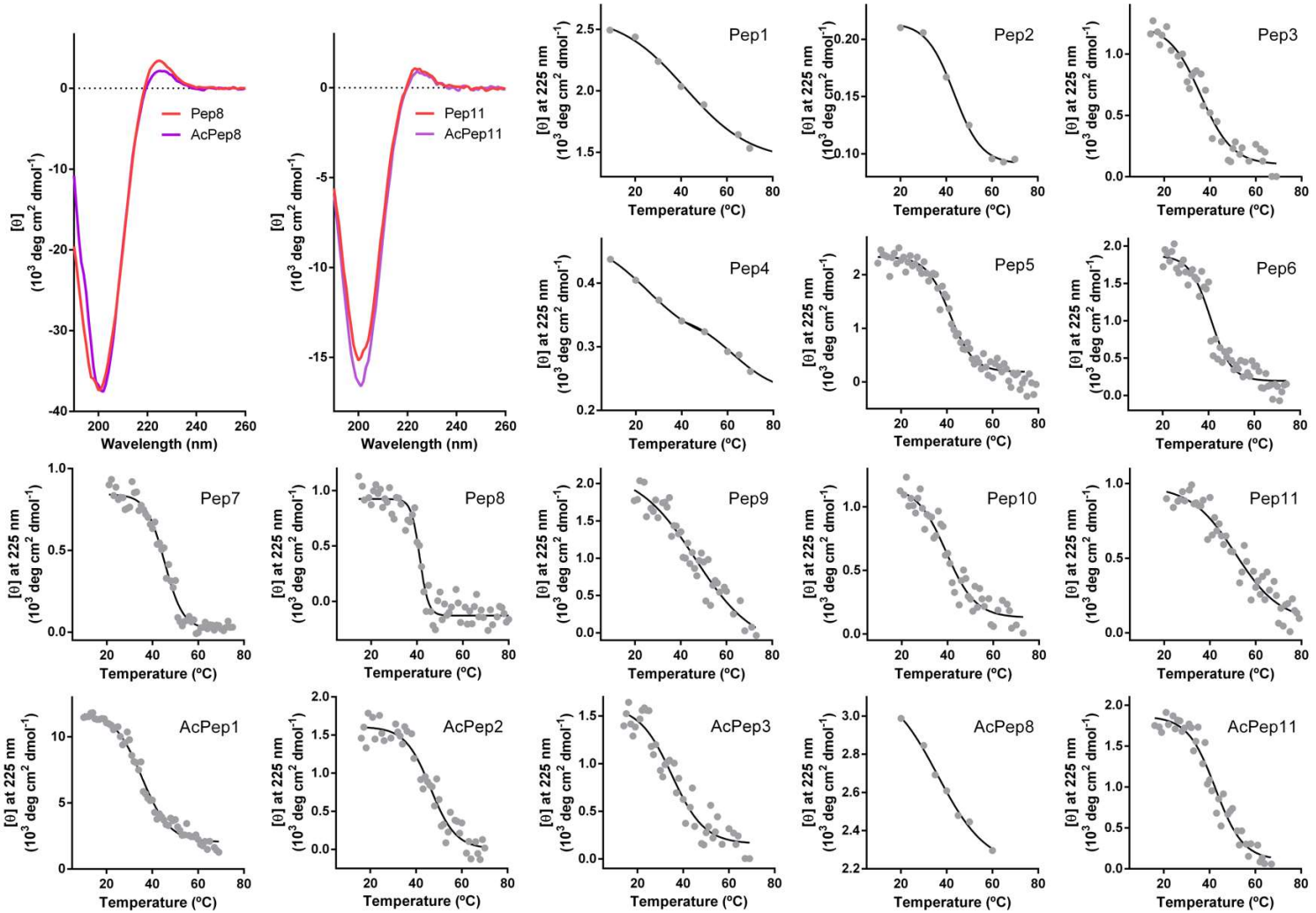

Supplementary Fig. 1. Engineered peptide sequences display CD spectra and melting curves typical of collagen-like peptides. Top left: CD spectra for selected peptides (Pep8, Pep11, AcPep8, and AcPep11) measured at 100 µM concentration in phosphate saline buffer (pH 7.4). The other plots in the figure correspond to melting curves measured for the 16 peptides at 225 nm scanned from 20 to 75 ºC. Curves were fitted using a sigmoidal model with $R^2 > 0.9$. All the CD raw data are available in Figshare: https://figshare.com/s/b8c4421feed97495ad43.

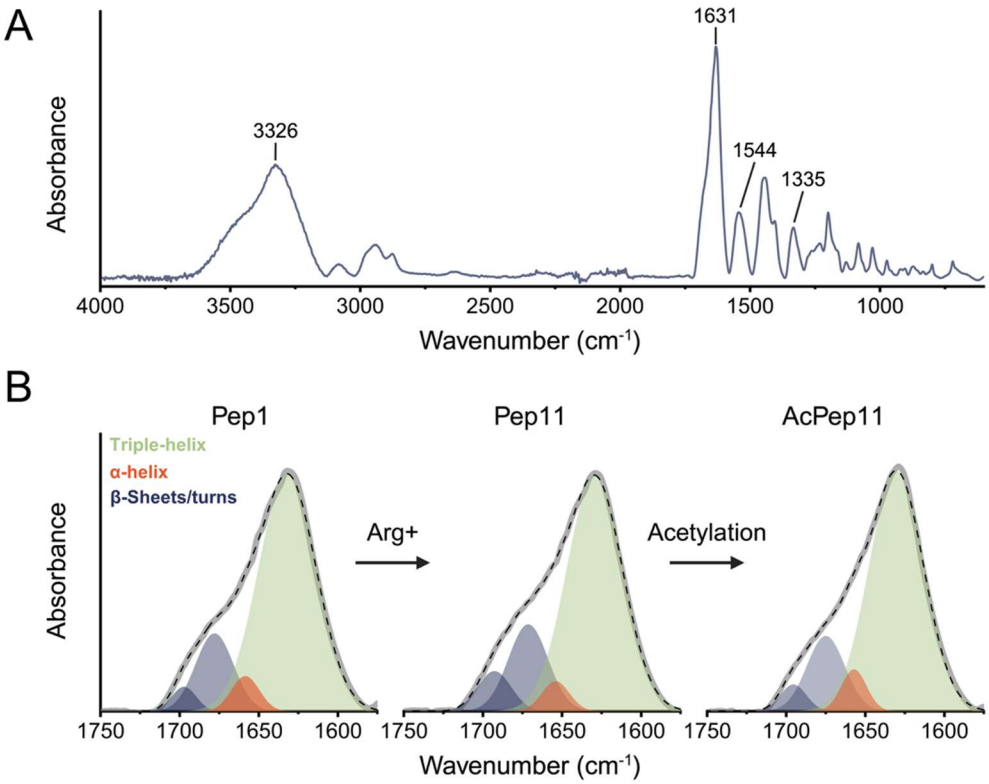

Supplementary Fig. 2. ATR-FTIR spectra of collagen-like peptides. A) ATR-FTIR of Pep1, which shows the characteristic peptide signals including N-H and O-H at 3326 cm^{-1}, amide I at 1631 cm^{-1}, amide II at 1544 cm^{-1}, and amide III at 1335 cm^{-1}. B) Gaussian fit analysis of the amide I signal for Pep1, Pep11, and AcPep11. Considering that the amide I region could be related to the backbone conformation of the peptide,[1,2] the deconvolution of this region was studied and compared. The results show different peaks, where the one shown in green is commonly attributed to the contribution of triple-helix structures.[3-5] Comparing the effect of changing Gly (Pep 1) to Arg (Pep11) and modifying the N-terminal by acetylation (AcPep11), the results demonstrate that all the peptides retain their triple-helix folding. All the FTIR raw data are available in Figshare: https://figshare.com/s/b8c4421feed97495ad43.

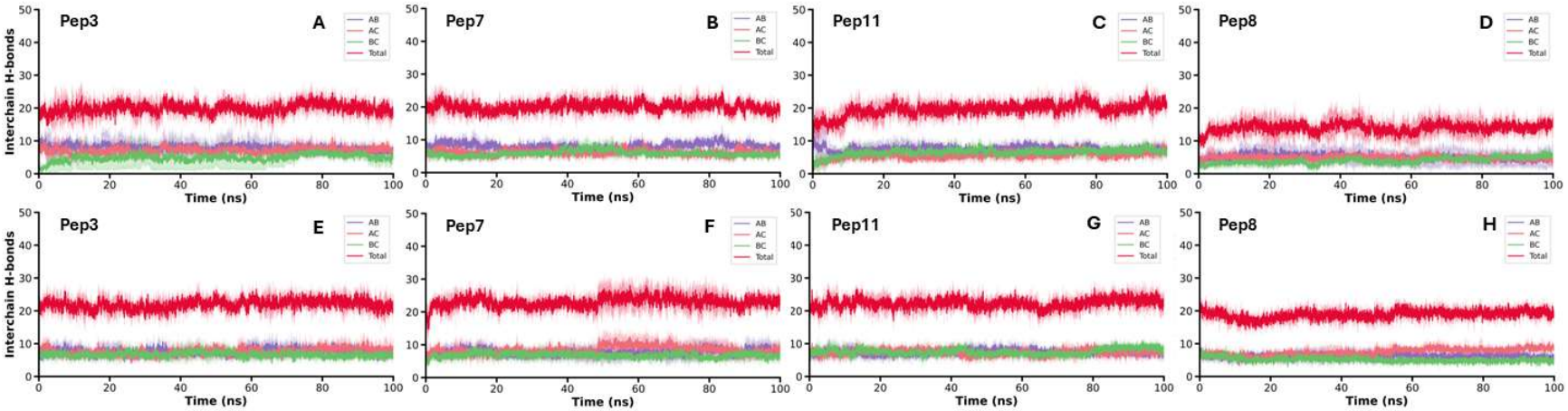

Supplementary Fig. 3. Interchain hydrogen-bond dynamics of collagen-like peptides in MD simulations started from stable and intermediate conformations. A) Time evolution of the average number of interchain H-bonds of Pep3 starting from the intermediate conformation. B) Time evolution of the average number of interchain H-bonds of Pep7 starting from the intermediate conformation. C) Time evolution of the average number of interchain H-bonds of Pep11 starting from the intermediate conformation. D) Time evolution of the average number of interchain H-bonds of Pep8 starting from the intermediate conformation. E) Time evolution of the average number of interchain H-bonds of Pep3 starting from the stable conformation. F) Time evolution of the average number of interchain H-bonds of Pep7 starting from the stable conformation. G) Time evolution of the average number of interchain H-bonds of Pep11 starting from the stable conformation. H) Time evolution of the average number of interchain H-bonds of Pep8 starting from the stable conformation. Total interchain interactions are shown in red, while the individual interchain contributions are displayed in green, pink, and grey. Peptides containing C-terminal arginines (Pep3, Pep7, Pep11) maintain H-bond counts throughout both simulations, consistent with their strong thermal stability. This interpretation is reinforced by the behavior of Pep8, which harbors arginine residues at the N-terminus and correspondingly exhibits diminished H-bond stability, highlighting the critical role of arginine positioning.

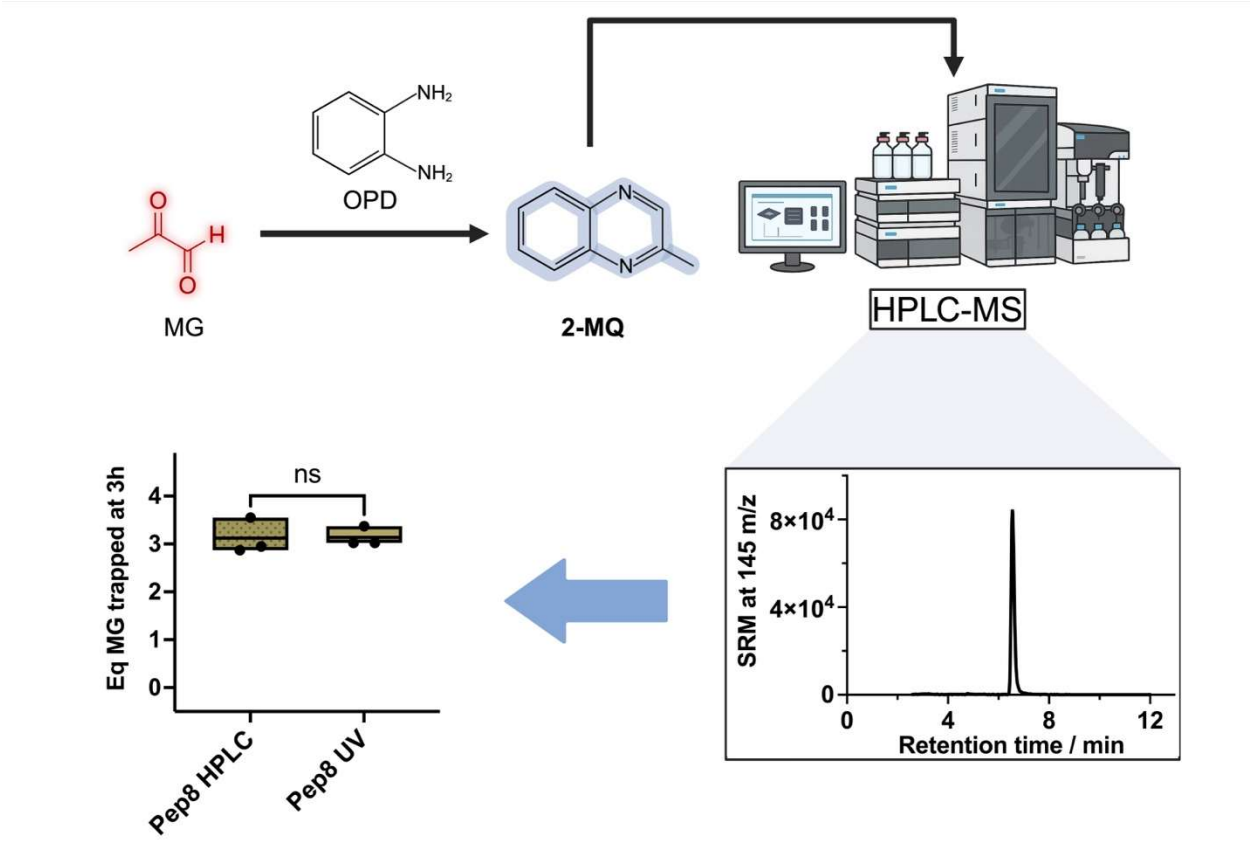

Supplementary Fig. 4. Schematic of the HPLC-MS quantification method. MG was derivatized with o-phenylenediamine (OPD) to yield 2-methylquinoxaline (2-MQ), which was assessed by HPLC-MS single-reaction monitoring at 145 m/z. The box-plot comparison of MG consumption for Pep8 by HPLC-MS versus spectrophotometry shows no significant differences between the 2 methods of analysis.

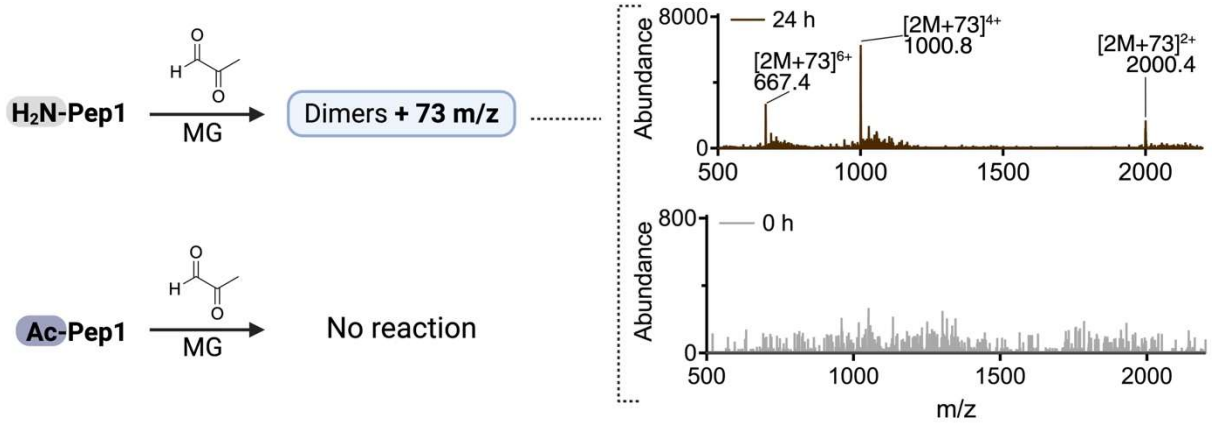

Supplementary Fig. 5. MG trapping by Pep1 via its N-terminal α-amine. Pep1 (250 µM) and AcPep1 (250 µM) were incubated with excess MG (5 mM) in 100 mM phosphate buffer (pH 7.4) for up to 24 h. HPLC-MS extracted-ion chromatograms showed a complete loss of Pep1 and no change in AcPep1. Top: Electrospray ionization mass spectrum (ESI-MS) at 24 h displaying a single product ion at m/z = 2 M + 73 (retention time 14.5 min), assigned to an MG-bridged peptide dimer (Pep1). Bottom: spectrum at 0 h, where this ion is absent (Pep1). No additional MG-derived adducts were detected, confirming that the free N-terminal α-amine is the only nucleophilic site under these conditions.

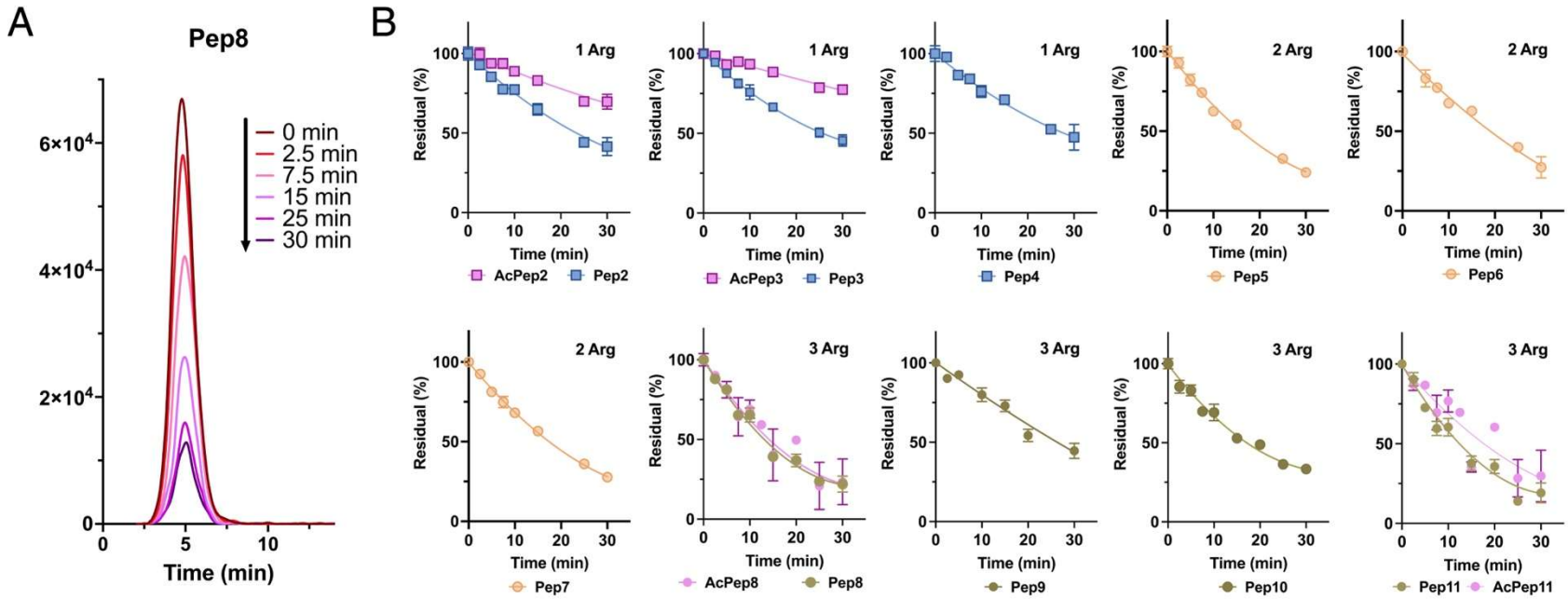

Supplementary Fig. 6. MG-dependent depletion kinetics of the arginine-containing collagen-like peptides. A) Representative extracted-ion chromatogram (EIC) for the $[M + 2H]^{2+}$ ion of Pep 8 (755 m/z) during a 0–30 min incubation with excess MG (5 mM) at an initial peptide concentration of 250 µM. B) Fraction of the peptide remaining vs. time for different peptides grouped by their number of arginine residues. Kinetic curves were obtained from EIC traces analogous to the sample shown in panel A and fitted to a pseudo-first-order exponential decay model (solid lines).

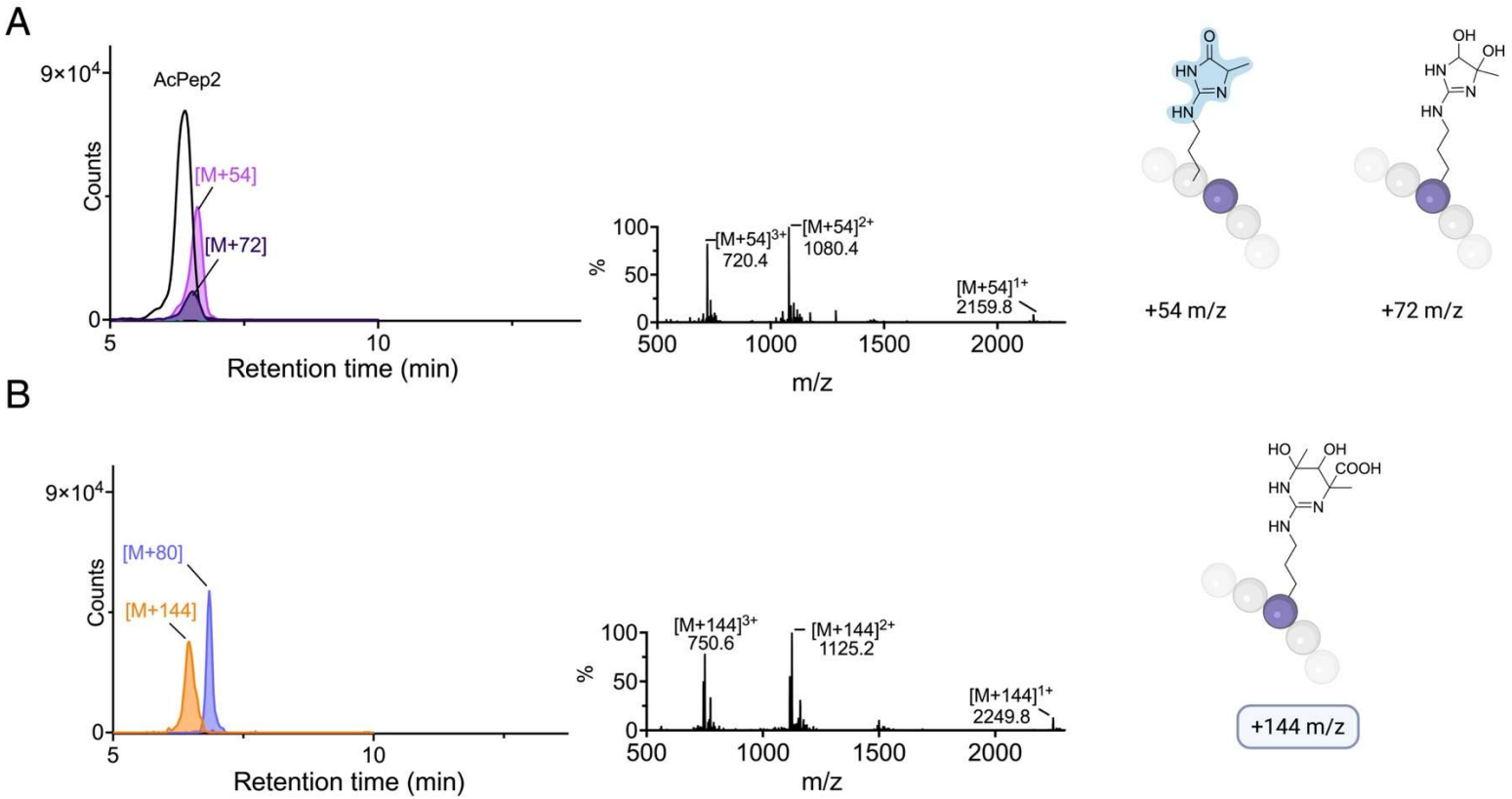

Supplementary Fig. 7. MG-derived products of AcPep2 identified by HPLC–MS. A) [*Left*]: Extracted-ion chromatograms (EICs) after 3 h incubation (250 µM peptide, 5 mM MG, pH 7.4, 37 °C) showing the parent ion (M) and mono-MG adducts at M + 54 and M + 72; and [*Right*] ESI-MS spectrum of the M + 54 peak and schematic representation of the two common mono-MG modifications. This confirmed the expected mass shift and is typical of the canonical hemithioacetal and imidazolone pathways.[6] B) [*Left*]: EICs obtained after 1 week: the parent peptide is absent, and only 2 di-MG adducts at M + 80 and M + 144 remained; and [*Right*]: MS spectrum of the M + 144 peak with its structure. This evolution from mono- to di-adducts is fully consistent with the MG-consumption profiles reported in Figure 3B.

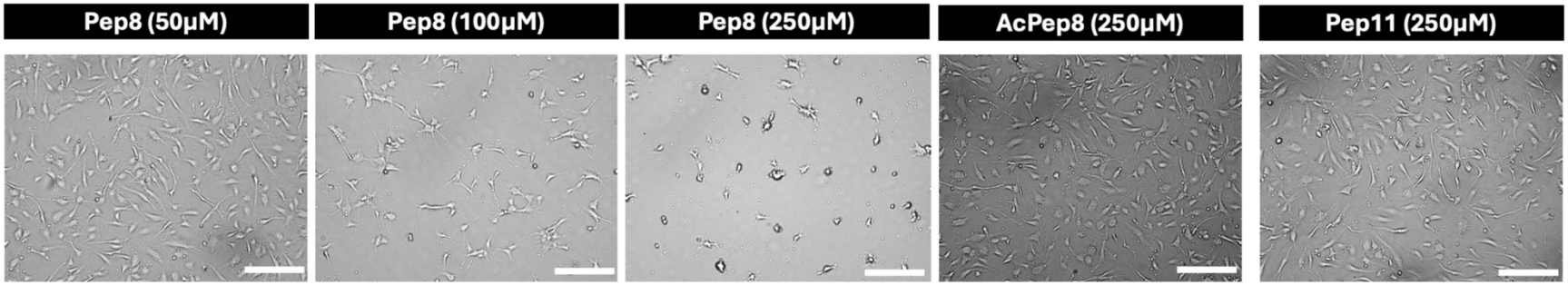

Supplementary Fig. 8. Acetylation of Pep8 reverses its *in vitro* cytotoxicity to endothelial cells. Representative images showing the morphology and number of human coronary microvascular endothelial cells (HCMECs) cultured with increasing concentrations of Pep8 for 24 h. Representative image of HCMECs treated with AcPep8 or Pep11 for 24 h. At higher concentrations (100 and 250 μM), Pep8 exhibited a toxic effect on the cells, which was not observed with treatment of a high concentration of AcPep8 or Pep11 (250 μM) (scale bar = 200 μm).

.

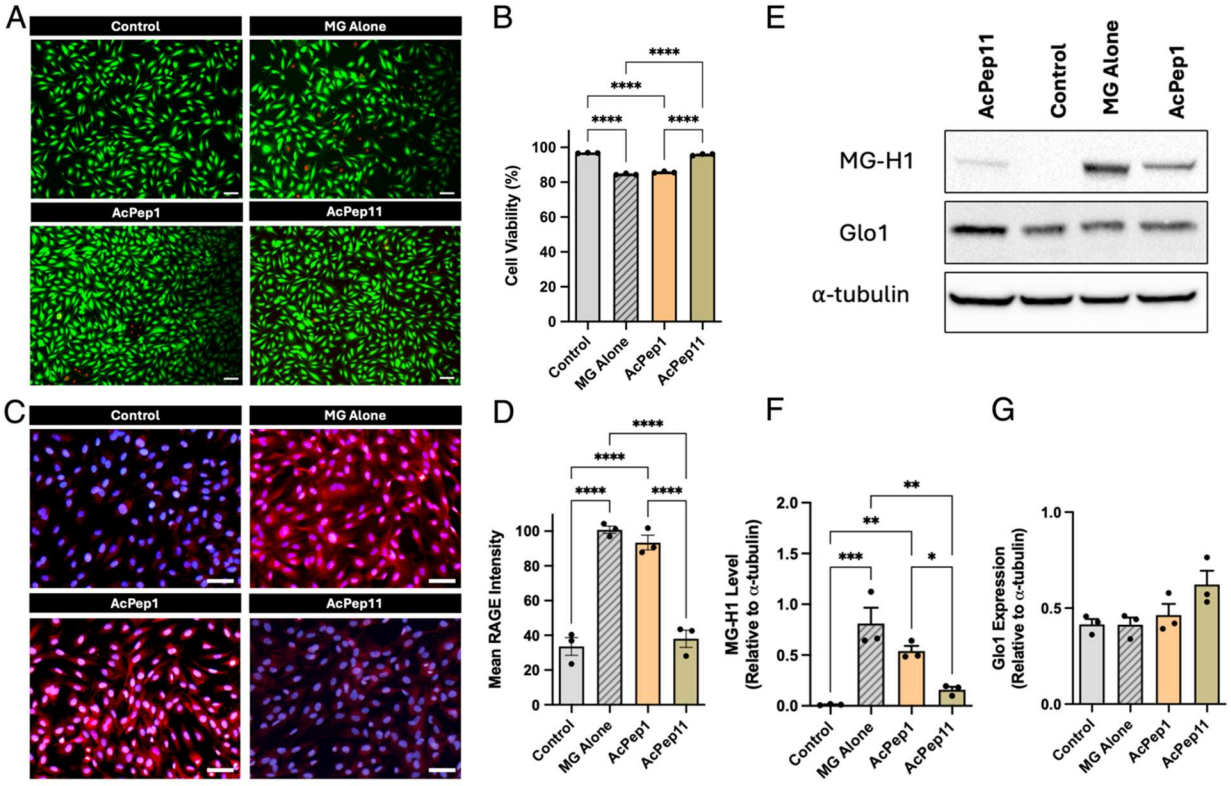

Supplementary Fig. 9. **AcPep11 treatment protects cells from MG damage *in vitro***. A) Representative Live/Dead assay images of HCMECs after 24 h of culture with 4 different treatments (scale bar =100 µm). B) Quantification of HCMEC viability ($n = 3$ per group). C) Representative immunofluorescence images of RAGE staining of HCMECs after 24 h of culture with 4 different treatments (scale bar = 50 µm). D) Quantification of the mean fluorescence intensity of RAGE. E) Representative western blot images for MG-H1 and Glo1 expression in HCMECs after 24 h of culture with 4 different treatments. Quantification of the western blot results for (F) MG-H1 and (G) Glo1 ($n = 3$ per group). Data are presented as the mean ± SEM. Differences between groups were determined by a one-way ANOVA with Bonferroni correction. *$p < 0.05$, **$p < 0.01$, ***$p < 0.001$, ****$p < 0.00001$.

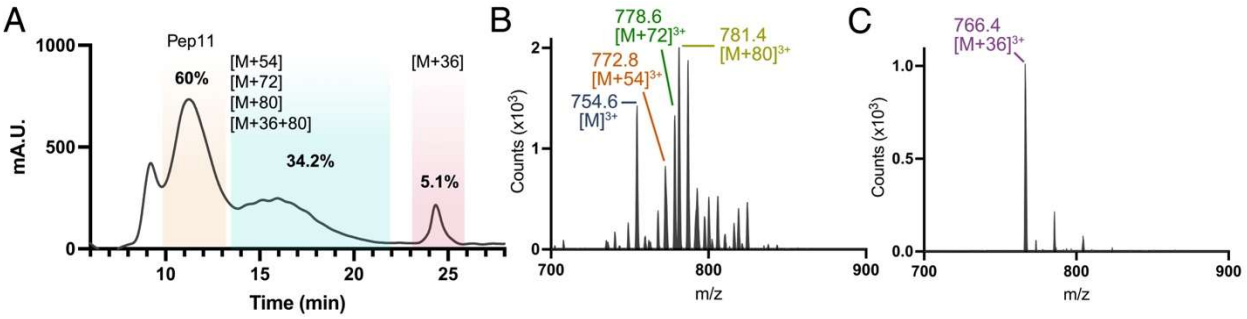

Supplementary Fig. 10. **HPLC-MS analysis for the detection of Pep11-AGEs after 24 h incubation of Pep11 with MG**. A) Pep11-AGEs chromatogram showing 3 different integration areas. B) Mass spectrometry signals between 700 – 900 m/z (rt= 13 – 20 min). C) Mass spectrometry signals between 700 – 900 m/z (rt= 21 – 26 min).

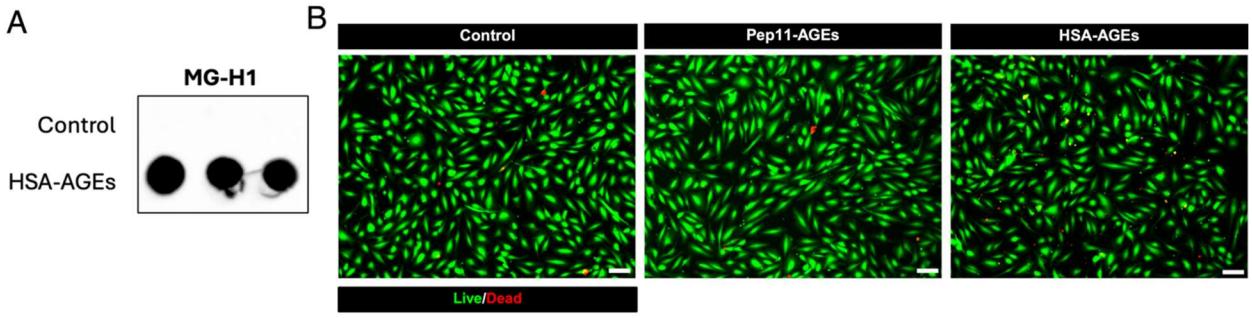

Supplementary Fig. 11. Pep11-AGEs showed no toxicity to endothelial cells. A) Dot blot analysis of HSA-AGEs for MG-H1. B) Representative Live/Dead assay images of HCMECs after 24 h of culture with 3 different conditions (scale bar = 100 μm).

Mass spectroscopy for each peptide

Pep1

Sequence	Molecular weight [g.mol^{-1}]	M+1H	M+2H
H_2N-GGG**(POG)$_6$**GGG-OH	1964.0	1964.9	982.8

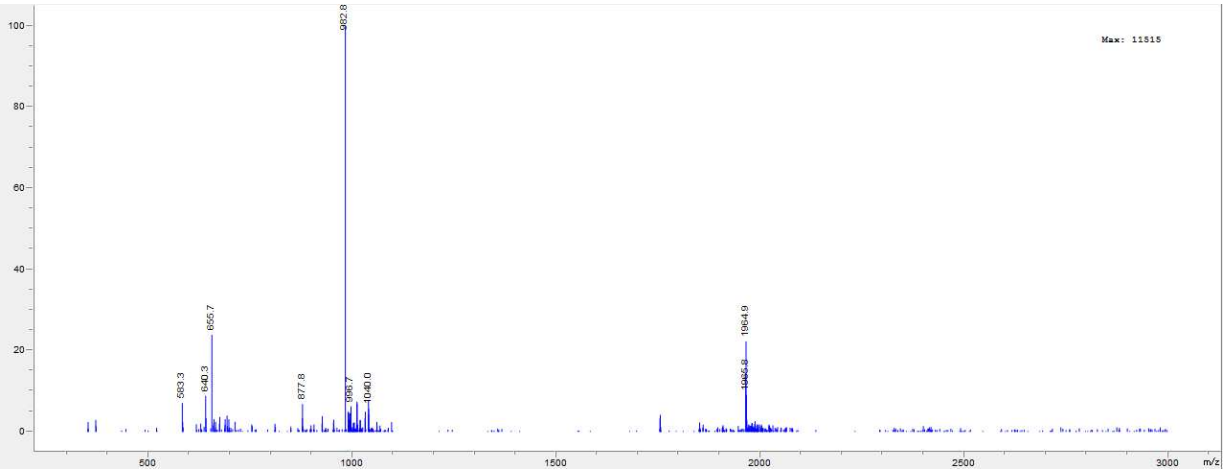

Pep2

Sequence	Molecular weight [g.mol^{-1}]	M+1H	M+2H
H_2N-GRG**(POG)$_6$**GGG-OH	2063.2	2064.2	1032.5

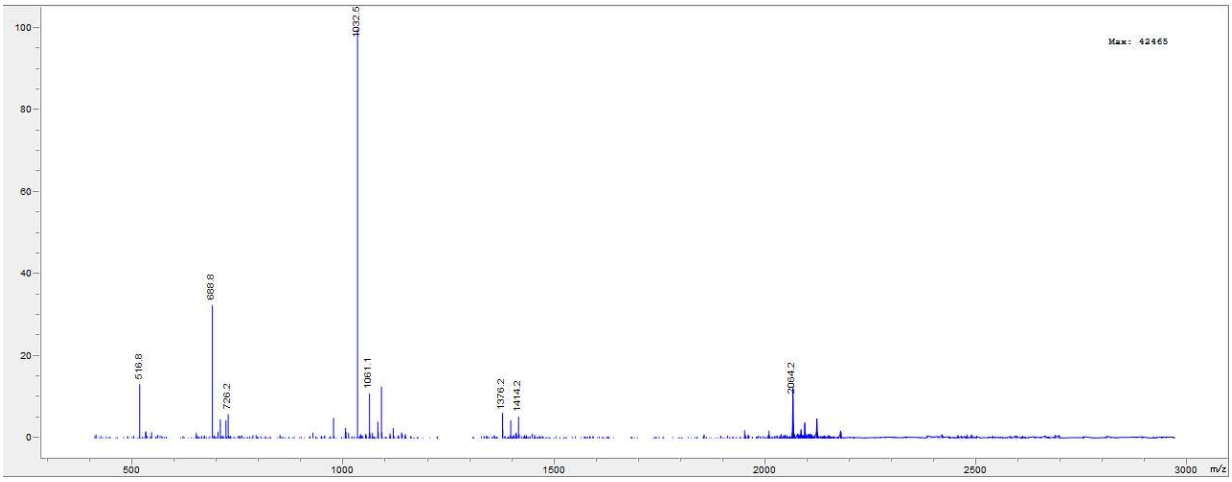

Pep3

Sequence	Molecular weight [g.mol^{-1}]	M+2H	M+3H
H_2N-GGG**(POG)$_6$**G**R**G-OH	2063.2	1032.3	688.7

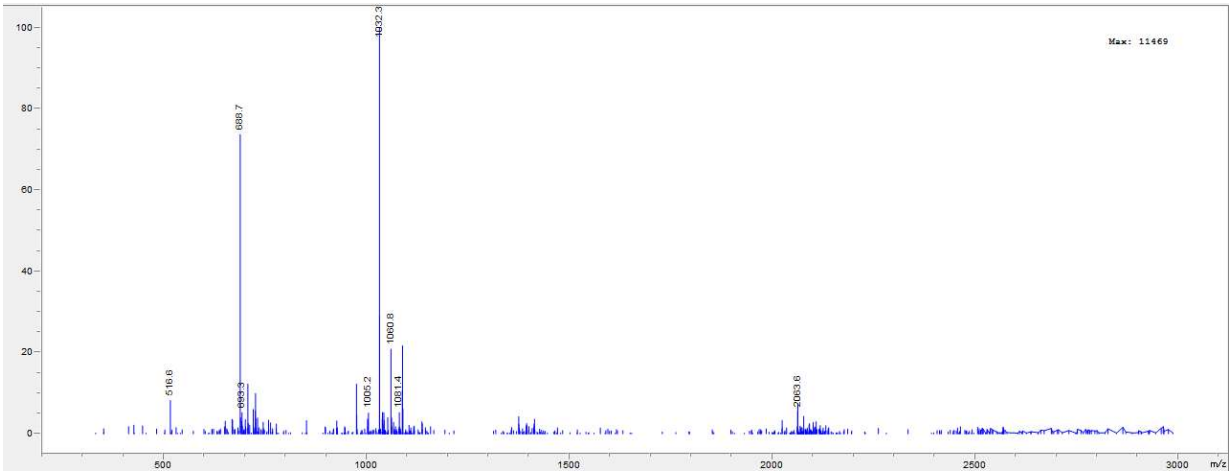

Pep4

Sequence	Molecular weight [g.mol^{-1}]	M+1H	M+2H
H_2N- GGG**(POG)2**(P**R**G)**(POG)3**GGG -OH	2007.1	1004.3	669.9

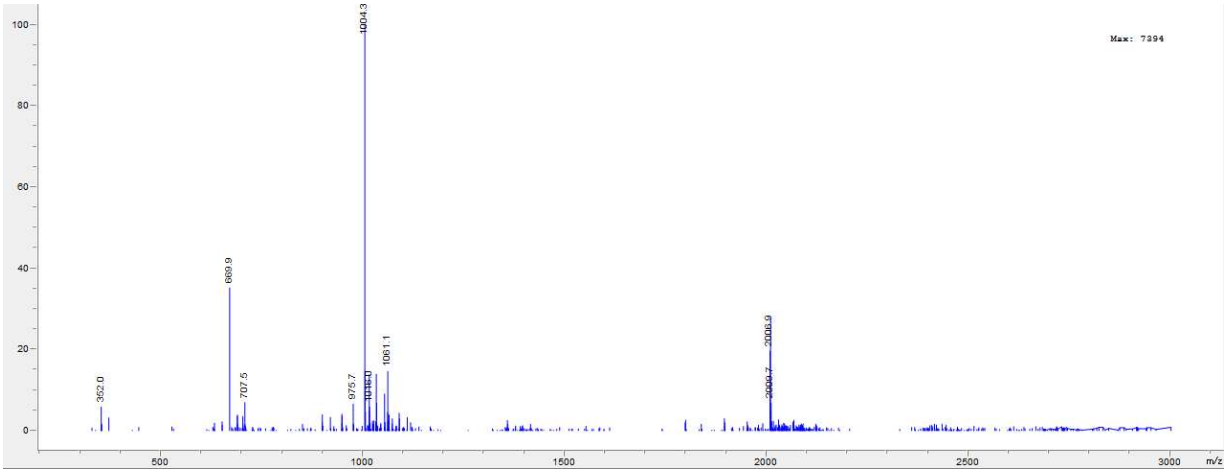

Pep5

Sequence	Molecular weight [g.mol^{-1}]	M+1H	M+2H
H_2N-**RR**G**(POG)$_6$**GGG-OH	2162.3	1082.1	721.8

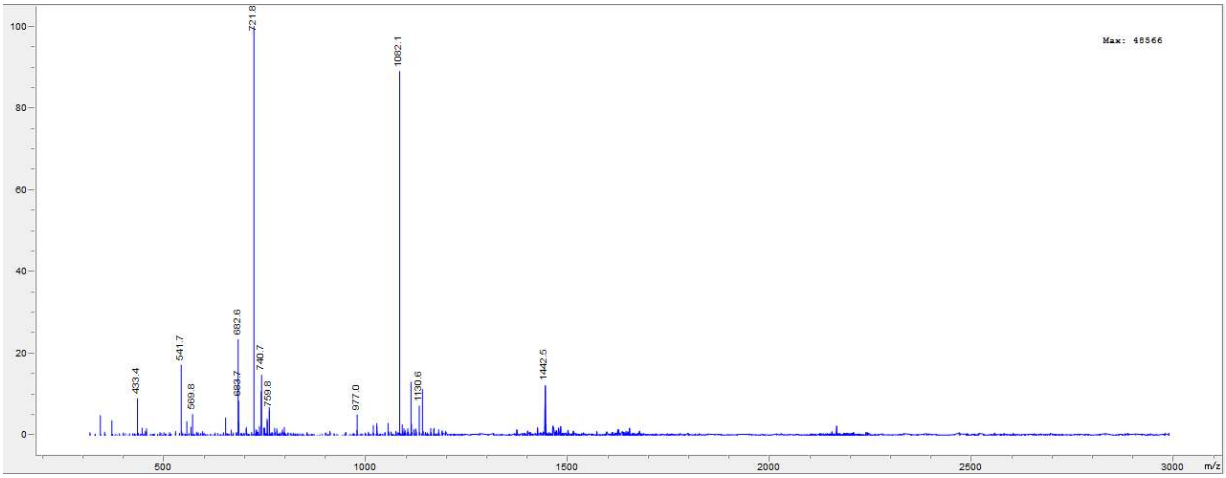

Pep6

Sequence	Molecular weight [g.mol^{-1}]	M+1H	M+2H
H_2N-GRG**(POG)$_6$**GRG-OH	2162.3	1082.1	721.8

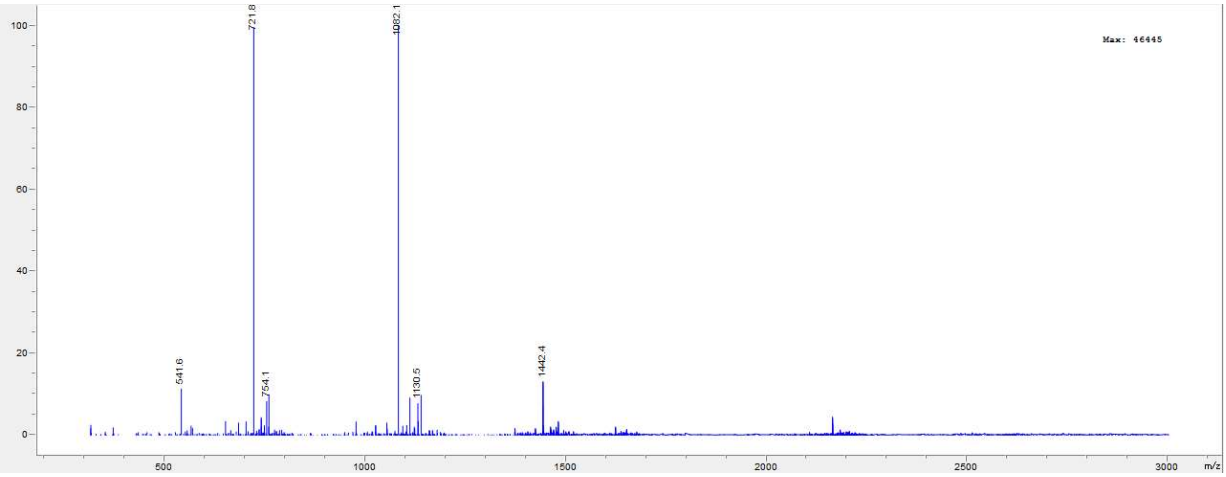

Pep7

Sequence	Molecular weight [g.mol^{-1}]	M+1H	M+2H
H_2N-GGG**(POG)$_6$**G**RR**-OH	2162.3	1081.9	721.8

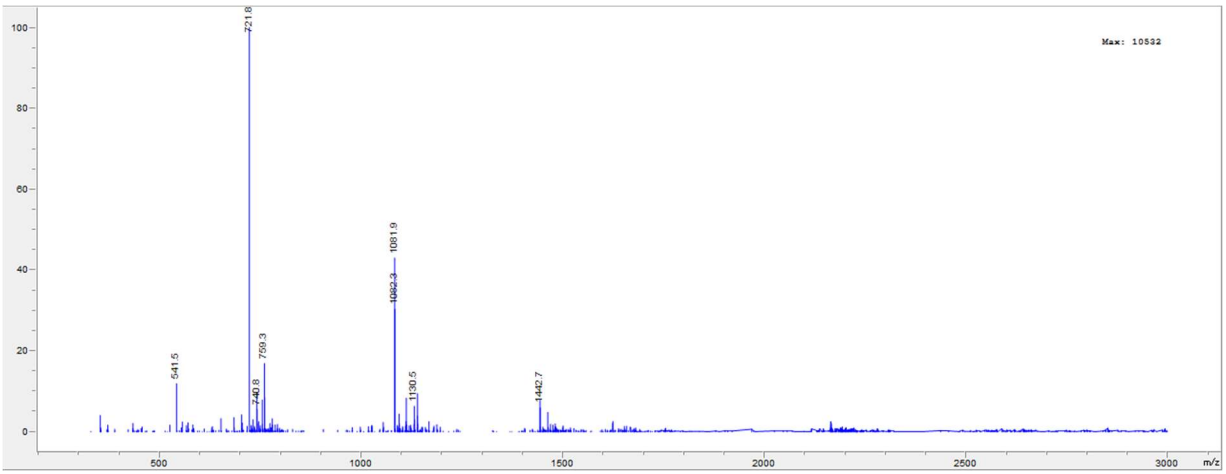

Pep8

Sequence	Molecular weight [g.mol^{-1}]	M+2H	M+3H
H_2N-**RRR(POG)$_6$**GGG-OH	2261.4	1131.6	754.9

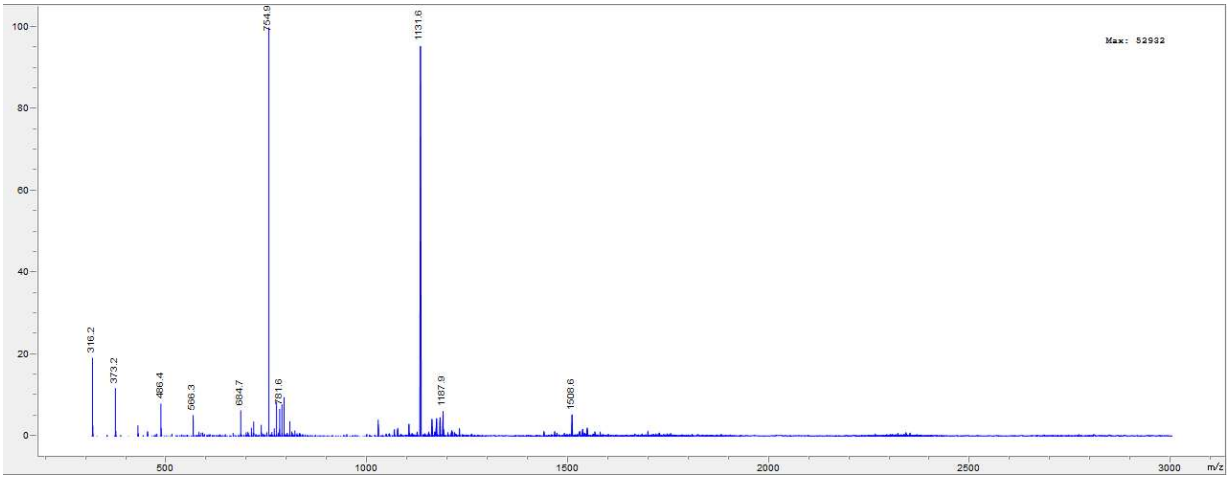

Pep9

Sequence	Molecular weight [g.mol^{-1}]	M+2H	M+3H
H_2N-**RR**G**(POG)$_6$**G**R**G-OH	2261.4	1131.5	754.8

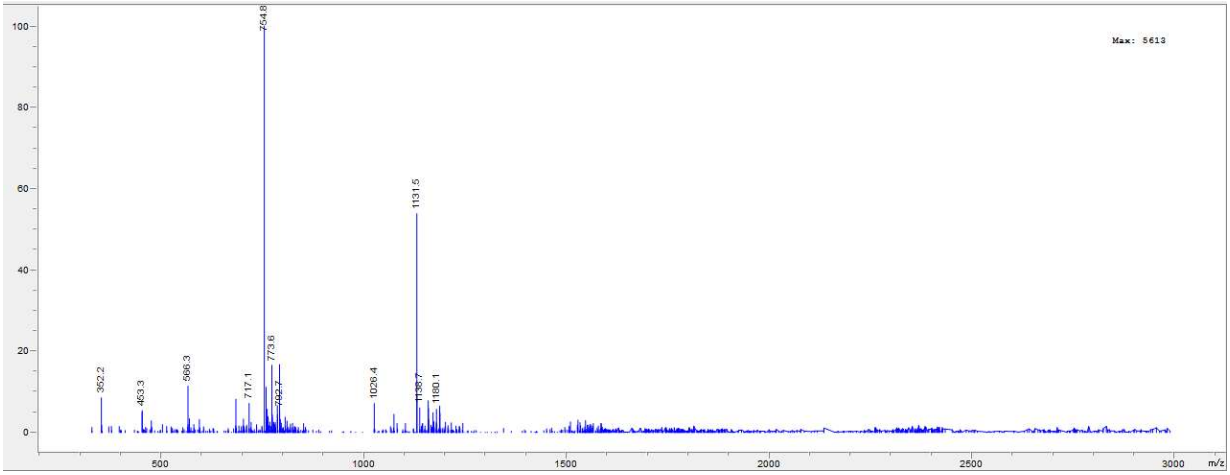

Pep10

Sequence	Molecular weight [g.mol^{-1}]	M+2H	M+3H
H_2N-GRG**(POG)$_6$**GRR-OH	2261.4	1131.9	754.8

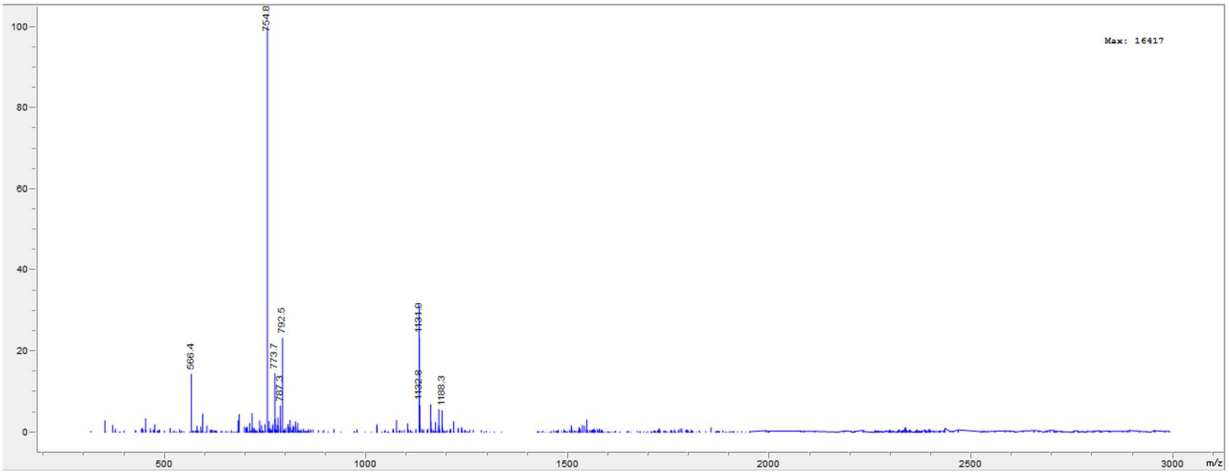

Pep11

Sequence	Molecular weight [g.mol^{-1}]	M+2H	M+3H
H_2N-GGG**(POG)$_6$**RRR-OH	2261.4	1131.3	754.7

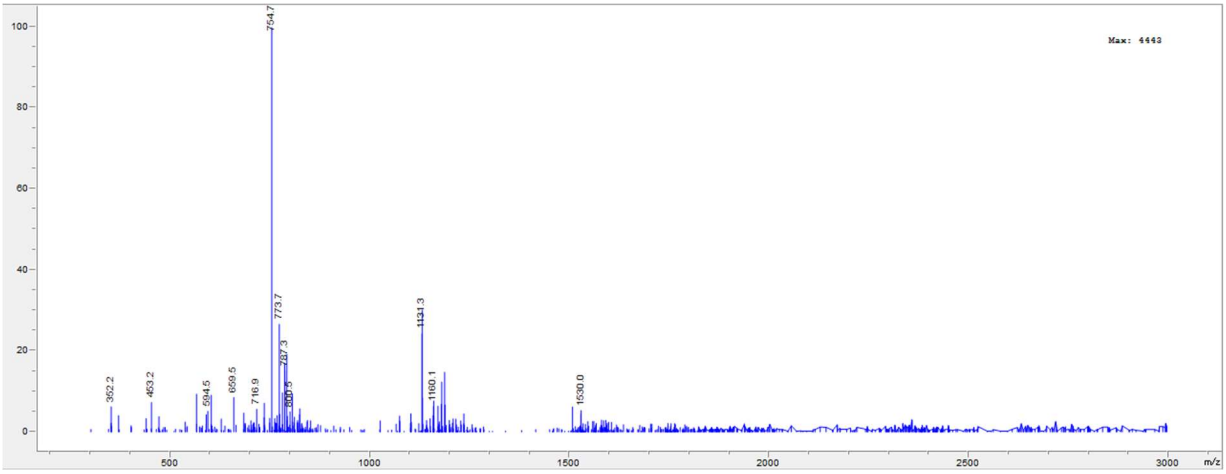

AcPep1

Sequence	Molecular weight [g.mol^{-1}]	M+2H
Ac-GGG**(POG)$_6$**GGG-OH	2006.1	1003.8

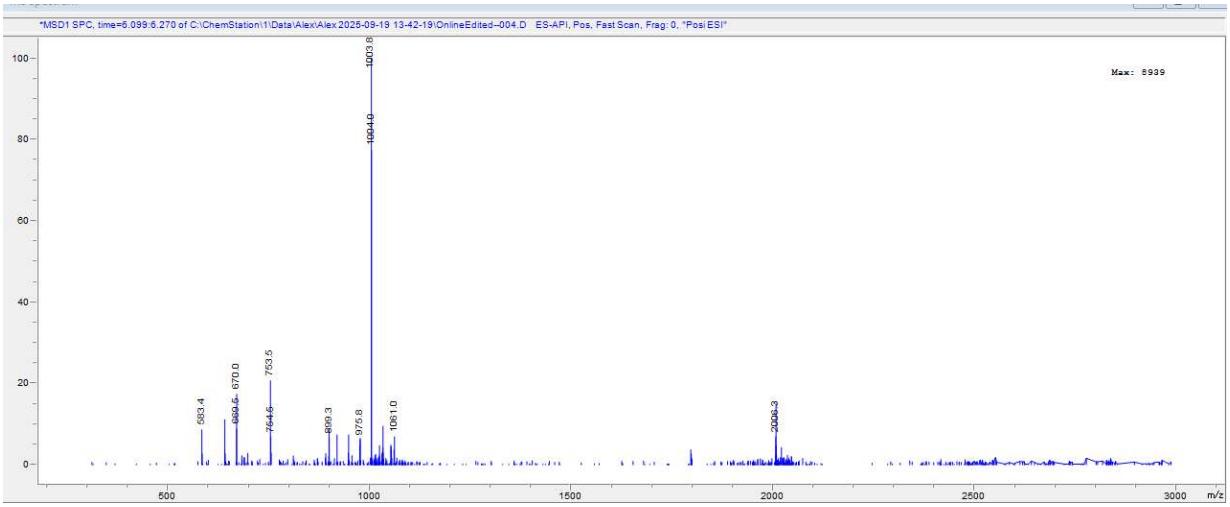

AcPep2

Sequence	Molecular weight [g.mol^{-1}]	M+2H	M+3H
Ac-G**R**G**(POG)$_6$**GGG-OH	2105.2	1053.6	702.8

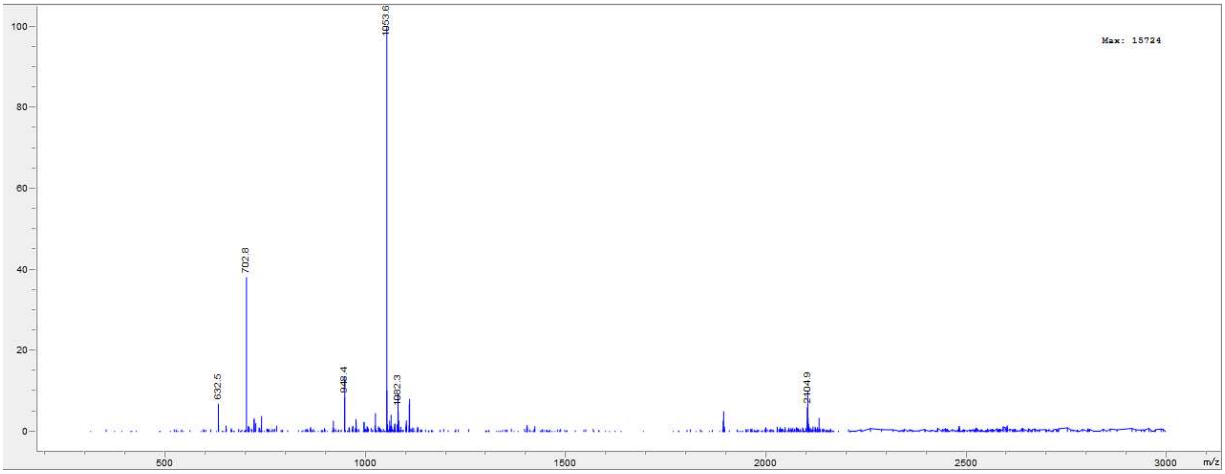

AcPep3

Sequence	Molecular weight [g.mol^{-1}]	M+2H	M+3H
Ac-GGG**(POG)$_6$**G**R**G-OH	2105.2	1053.2	702.4

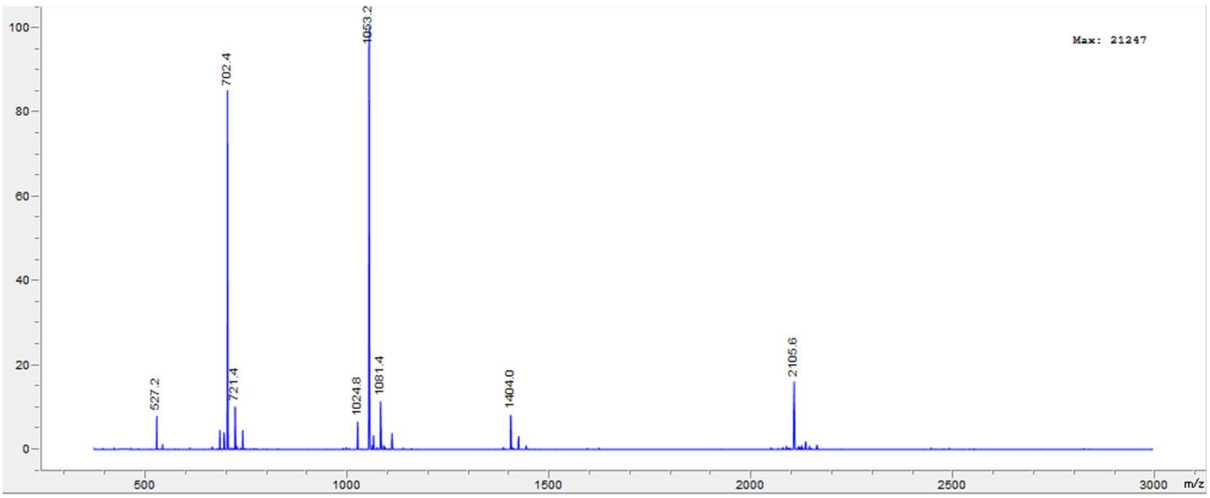

AcPep8

Sequence	Molecular weight [g.mol^{-1}]	M+2H	M+3H
Ac-**RRR(POG)$_6$**GGG-OH	2303.5	1152.4	768.4

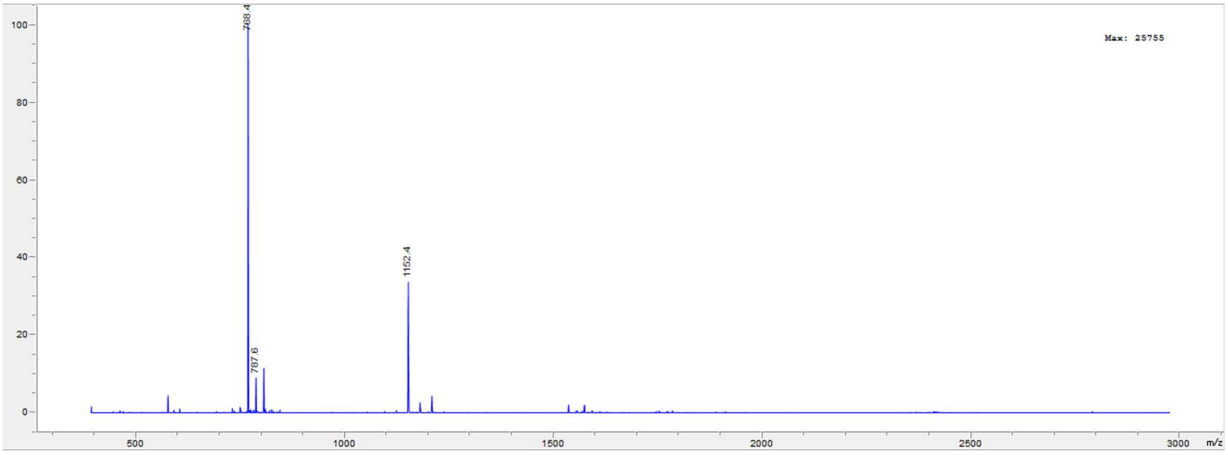

AcPep11

Sequence	Molecular weight [g.mol^{-1}]	M+2H	M+3H
Ac-GGG**(POG)$_6$RRR**-OH	2303.5	1152.9	768.9

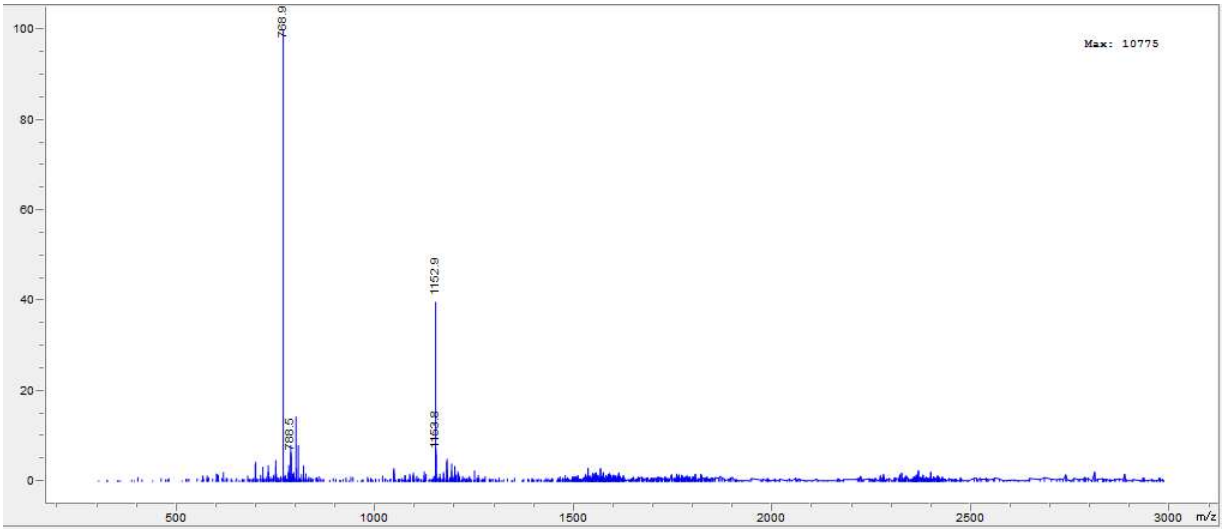

References

1 Ji, W. *et al.* Stoichiometry-controlled secondary structure transition of amyloid-derived supramolecular dipeptide co-assemblies. *Commun. Chem.* **2**, 65 (2019).

2 Castro, V. I. B. *et al.* Glycopeptide-based supramolecular hydrogels induce differentiation of adipose stem cells into neural lineages. *ACS Appl. Mater. Interfaces* **15**, 29998-30007 (2023).

3 Belbachir, K., Noreen, R., Gouspillou, G. & Petibois, C. Collagen types analysis and differentiation by FTIR spectroscopy. *Anal. Bioanal. Chem.* **395**, 829-837 (2009).

4 Terzi, A. *et al.* Effects of processing on structural, mechanical and biological properties of collagen-based substrates for regenerative medicine. *Sci. Rep.* **8**, 1429 (2018).

5 Barreto, M. S. C., Elzinga, E. J. & Alleoni, L. R. F. The molecular insights into protein adsorption on hematite surface disclosed by in-situ ATR-FTIR/2D-COS study. *Sci. Rep.* **10**, 13441 (2020).

6 McEwen, J. M., Fraser, S., Guir, A. L. S., Dave, J. & Scheck, R. A. Synergistic sequence contributions bias glycation outcomes. *Nat. Commun.* **12**, 3316 (2021).